



THE UNIVERSITY *of* EDINBURGH

Edinburgh Research Explorer

An Experimental Investigation on the Kinetics of Integrated Methane Recovery and CO₂ Sequestration by Injection of Flue Gas into Permafrost Methane Hydrate Reservoirs

Citation for published version:

Hassanpouryouzband, A, Yang, J, Okwananke, A, Burgass, R, Tohidi, B, Chuvilin, E, Istomin, V & Bukhanov, B 2019, 'An Experimental Investigation on the Kinetics of Integrated Methane Recovery and CO₂ Sequestration by Injection of Flue Gas into Permafrost Methane Hydrate Reservoirs', *Scientific Reports*. <https://doi.org/10.1038/s41598-019-52745-x>

Digital Object Identifier (DOI):

[10.1038/s41598-019-52745-x](https://doi.org/10.1038/s41598-019-52745-x)

Link:

[Link to publication record in Edinburgh Research Explorer](#)

Document Version:

Publisher's PDF, also known as Version of record

Published In:

Scientific Reports

Publisher Rights Statement:

© The Author(s) 2019

General rights

Copyright for the publications made accessible via the Edinburgh Research Explorer is retained by the author(s) and / or other copyright owners and it is a condition of accessing these publications that users recognise and abide by the legal requirements associated with these rights.

Take down policy

The University of Edinburgh has made every reasonable effort to ensure that Edinburgh Research Explorer content complies with UK legislation. If you believe that the public display of this file breaches copyright please contact openaccess@ed.ac.uk providing details, and we will remove access to the work immediately and investigate your claim.



OPEN

An Experimental Investigation on the Kinetics of Integrated Methane Recovery and CO₂ Sequestration by Injection of Flue Gas into Permafrost Methane Hydrate Reservoirs

Aliakbar Hassanpouryouzband^{1,2}, Jinhai Yang^{1*}, Anthony Okwananke¹, Rod Burgass¹, Bahman Tohidi¹, Evgeny Chuvilin³, Vladimir Istomin³ & Boris Bukhanov³

Large hydrate reservoirs in the Arctic regions could provide great potentials for recovery of methane and geological storage of CO₂. In this study, injection of flue gas into permafrost gas hydrates reservoirs has been studied in order to evaluate its use in energy recovery and CO₂ sequestration based on the premise that it could significantly lower costs relative to other technologies available today. We have carried out a series of real-time scale experiments under realistic conditions at temperatures between 261.2 and 284.2 K and at optimum pressures defined in our previous work, in order to characterize the kinetics of the process and evaluate efficiency. Results show that the kinetics of methane release from methane hydrate and CO₂ extracted from flue gas strongly depend on hydrate reservoir temperatures. The experiment at 261.2 K yielded a capture of 81.9% CO₂ present in the injected flue gas, and an increase in the CH₄ concentration in the gas phase up to 60.7 mol%, 93.3 mol%, and 98.2 mol% at optimum pressures, after depressurizing the system to dissociate CH₄ hydrate and after depressurizing the system to CO₂ hydrate dissociation point, respectively. This is significantly better than the maximum efficiency reported in the literature for both CO₂ sequestration and methane recovery using flue gas injection, demonstrating the economic feasibility of direct injection flue gas into hydrate reservoirs in permafrost for methane recovery and geological capture and storage of CO₂. Finally, the thermal stability of stored CO₂ was investigated by heating the system and it is concluded that presence of N₂ in the injection gas provides another safety factor for the stored CO₂ in case of temperature change.

The oceans, permafrost regions, and continental and marine sediments contain a huge volume of methane trapped in the form of gas hydrates¹ which could be a potential energy source² or CO₂ storage sink³, depending upon human actions, with respect to energy policy and anthropogenic global warming. These ice-like hydrates which are non-stoichiometric inclusion compounds with hydrogen bonded water cages enclathrated light guest molecules without chemical bonds⁴, require suitable thermodynamic conditions including pressure, temperature, and surrounding liquid and gas compositions to remain stable. Various approaches were taken to shift the system conditions away from equilibrium in investigations of methane extraction from hydrate-bearing sediments. In comparison with potential methods such as thermal stimulation⁵, depressurization⁶, chemical inhibitor

¹Hydrates, Flow Assurance & Phase Equilibria Research Group, Institute of Petroleum Engineering, School of Energy, Geoscience, Infrastructure and Society, Heriot-Watt University, Riccarton, Edinburgh, EH14 4AS, UK. ²School of Geosciences, University of Edinburgh, Grant Institute, West Main Road, Edinburgh, EH9 3JW, UK. ³Skolkovo Institute of Science and Technology (Skoltech), 3 Nobel Street, Skolkovo Innovation Center, 10, Moscow, 143026, Russia. *email: petjy@hw.ac.uk

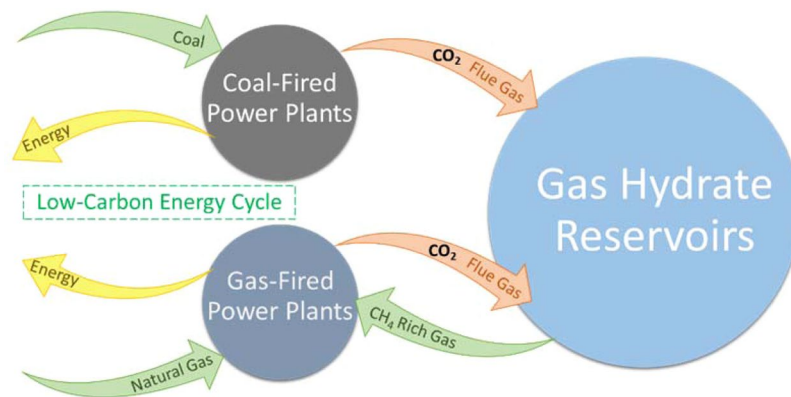


Figure 1. Graphical illustration of direct flue gas injection into hydrate-bearing sediments for geological carbon dioxide sequestration and methane recovery.

injection⁷, CO₂^{8,9} or CO₂-mixed gases¹⁰ (e.g., flue gas) injection is more environmentally friendly because of the potential to capture CO₂ simultaneously with methane recovery. Moreover, injection of CO₂-mixed gases (mainly CO₂ + N₂) produced directly from power stations rather than pure CO₂ is more economic owing to significant reductions in the total cost by avoidance of CO₂ separation cost^{10–12} (See Fig. 1).

Coal-fired power plants represent a substantial proportion of global anthropogenic CO₂ emissions which are the key contributors to global climate change¹³. The emission of CO₂ in pulverized coal plants is caused by combustion of air and coal in a boiler to generate energy, producing flue gas with a low concentration of CO₂ (~14%). Emission of flue gas from a typical 600 MWE power plant could be more than 500 m³ every second¹⁴. Accordingly, up-scaling post-combustion CO₂ capture from power-plant flue gas through sustainable methods is gaining importance, to limiting CO₂ emissions.

Previously, we presented initial results for injection of power-plant flue gas into gas hydrate reservoirs¹⁵ above freezing temperatures, defining a method¹⁰ to determine the optimum pressure for injection, where a more detailed review of the past literature can be found. In recent years, several^{12,16–18} investigations addressing various aspects of methane recovery by direct injection of flue gas have been reported, including limitations of CO₂/CH₄, effects of methane hydrate morphology and ratio of CO₂/N₂ in the injection gas¹⁷, the effect of sandstone permeability¹⁹, and efficiency of the method in the association with thermal stimulation¹². Here, referring to the companion papers^{10,15} as a basis for our interpretations where necessary, we report new experimental results for the kinetics of optimized flue gas injection into methane hydrate reservoirs at sub-zero temperatures, covering both sub glacial and permafrost conditions, in addition to further discussing previous results. The efficiency of the method at sub-zero temperatures was also investigated as a considerable proportion of gas hydrate reservoirs are located underneath permafrost formations^{20–22}. In addition, our previous experiments above freezing point showed significantly more favourable results for both CO₂ storage and methane recovery at lower temperatures, also emphasizing the necessity of investigating the method efficiency under 0 °C. One of the objectives of this study was to investigate the efficiency of the method (i.e., methane recovery and CO₂ storage percentages) in a realistic time scale and at hydrate reservoir conditions. The second key objective was to evaluate the impact of reservoir conditions on the kinetic efficiency, to examine potential methane reservoirs and identify a suitable site. Finally, the impact of global warming and natural temperature cycles on the stored CO₂ was also investigated with the aim of understanding potential environmental hazards.

Results and Discussion

Kinetics of CO₂ capture and CH₄ recovery at optimum pressure. Figure 2a–f show the changes in gas phase composition with time and pressure obtained by GC after flue gas was injected. As shown in Fig. 2a,b methane concentration and CO₂/(CO₂ + N₂) ratio changes with pressure in all experiments following a similar pattern. However there were differences in the rate of change, especially for those experiments conducted at temperatures below 0 °C. Initially, these values fluctuate slightly as a consequence of the initial pressure reduction, made in order to set the system at target pressure. Methane concentration in the gas phase increases continuously and the CO₂/(CO₂ + N₂) reduces at the target pressure until the system reaches equilibrium, as is indicated in circles in Fig. 2a,b. Gas concentration changes with time since the pressure set was plotted at Fig. 2c–f. The main mechanism involved is the chemical potential shift of the system to higher pressure after flue gas injection (see EXPERIMENTAL SECTION), which forces the methane molecules vacate the clathrate cages allowing CO₂ molecules to enter. This could either occur through CO₂ replacement or full/part dissociation of the existing methane hydrates and formation of new CO₂ or CO₂-mixed hydrates with an accompanying release of hydrogen-bonded water molecules. Considering the experimental conditions, formation of CO₂, CO₂-N₂, CO₂-CH₄, CO₂-N₂-CH₄, and N₂-CH₄ is possible from a thermodynamic point of view as the pressure in all the experiments is well inside the aforementioned hydrate stability zones (see EXPERIMENTAL SECTION).

Here, we define half-time ($t_{1/2}$) as the time required for half of the increase in methane concentration to occur between when the pressure is set and the final equilibrium point. The defined half-time, $t_{1/2}$ qualitatively reflects the economic viability of the proposed process for certain reservoirs, as for a reservoir with too high ($t_{1/2}$) industrial scale application of the method would not be possible. $t_{1/2}$ for all of the experiments was calculated to

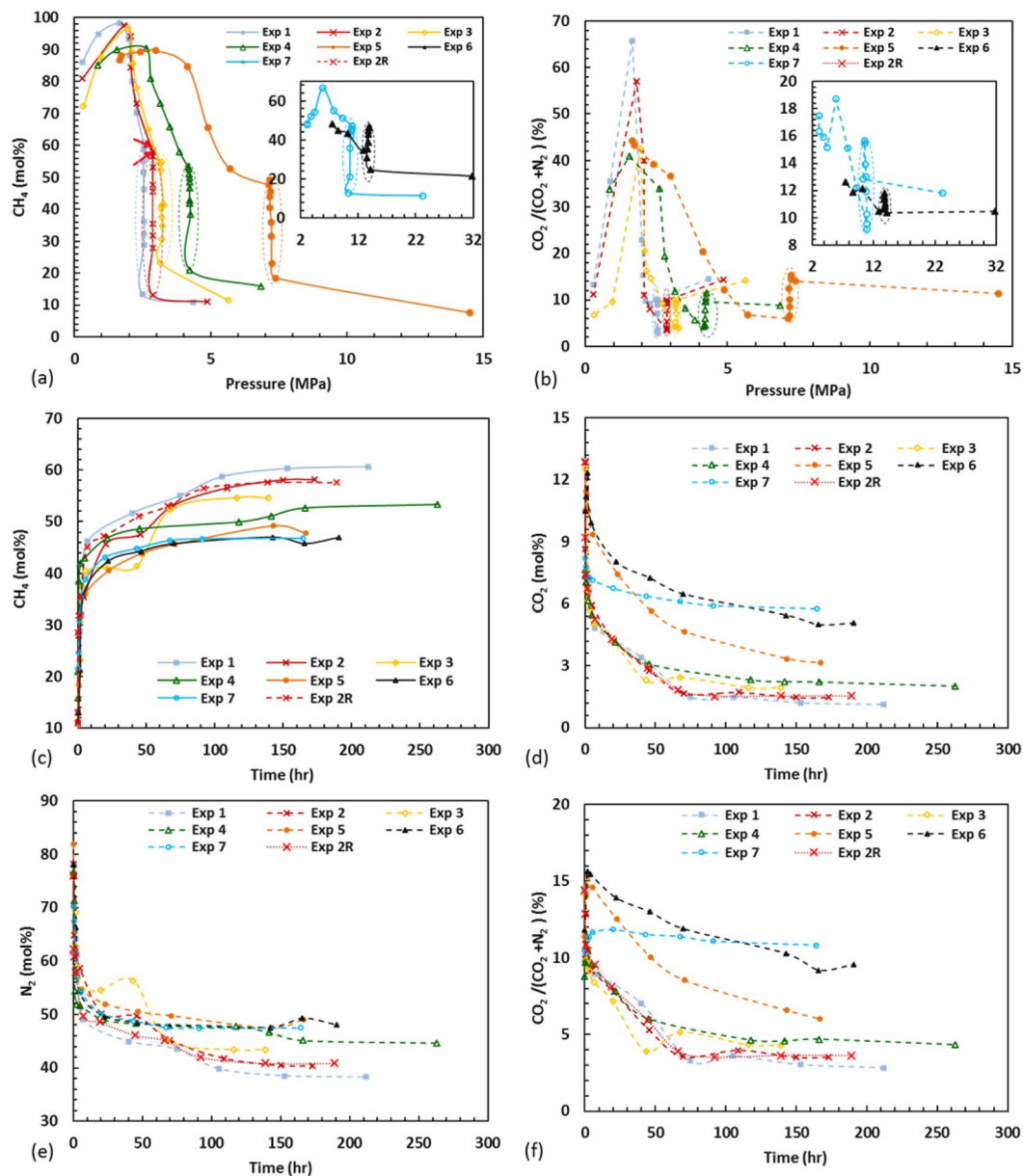


Figure 2. (a) CH_4 concentration and (b) $\text{CO}_2 / (\text{CO}_2 + \text{N}_2)$ evolution with pressure after flue gas was injected. CH_4 (c), CO_2 (d), N_2 (e), and $\text{CO}_2 / (\text{CO}_2 + \text{N}_2)$ evolution with time after pressure was set to the optimum value.

be no longer than 3 hours whereas the overall process could take up to 250 hours, indicating higher driving force due to higher chemical potential difference between gas and hydrate phase at the initial stage. A similar trend for the concentration of CO_2 and N_2 in the gaseous phase was observed (see Fig. 2d). At the later stage, increase of methane concentration in the gaseous phase dilutes CO_2 and N_2 concentration and consequently reduces the driving force for removing the CH_4 molecules from the hydrate phase. It is also possible that replacement occurs rapidly on the surface of the methane hydrate, then the replacement rate decelerates considerably because of formation of a CO_2 - CH_4 or CO_2 - N_2 hydrate (CNH) layer on the surface, acting as a physical barrier. This layer prevents the CO_2 molecules from entering into the interior of the methane hydrate, slowing down the replacement process. Thus, after forming a layer of CO_2 - CH_4 or CNH, replacement slows down and a limited diffusion transport becomes the main mechanism for the replacement process. A similar explanation was presented in the literature^{23–25}.

It is known that during formation of CO_2 - N_2 mixed hydrate, CO_2 goes to the large cavities, whereas N_2 will fill the small cavities²⁶. To examine the selectivity of the CO_2 over N_2 , $\text{CO}_2 / (\text{CO}_2 + \text{N}_2)$ ratio with time after pressure set is presented in Fig. 2f showing a decrease with time, indicating stronger selectivity of the CO_2 over N_2 in all the experiments owing to relatively higher^{27,28} stability of CO_2 than N_2 at the hydrate phase. This shows relatively higher occupancy of large cavities than small cavities. These results are in agreement with previous studies^{15,29}.

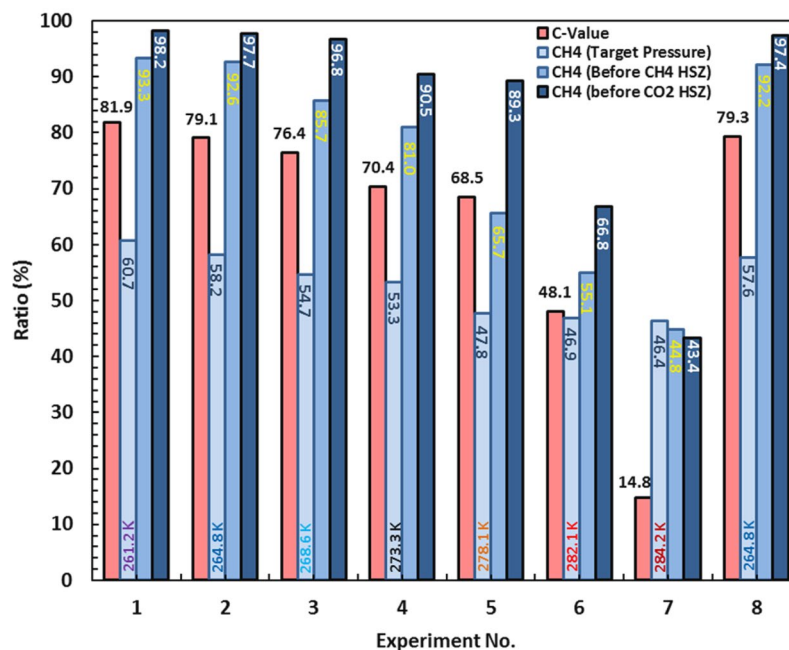


Figure 3. Calculated C-value, and CH₄ concentration at the optimum pressures after the system reached to the equilibrium and CH₄ concentration just before the system passed outside the CH₄ HSZ and CO₂ HSZ.

Methane recovery during depressurisation. As mentioned in the previous section the system was depressurized stepwise every 24 hours after reaching equilibrium state at the target pressure. As shown in Fig. 2a, as the system pressure reduces, CH₄ comes out of the hydrate phase and the percentage of CH₄ in the gas phase increases until reaching the CO₂ HSZ, after which CH₄ started to decrease because of dissociation of the CO₂ rich clathrates. This is true apart from Experiment 7, where CH₄ in the gas phase increases after initial drop. This can be attributed to the fact that in this experiment the pressure of the CO₂ hydrate dissociation is higher than that of CH₄ hydrate (see EXPERIMENTAL SECTION), thus, CO₂-rich hydrates dissociate first, followed by dissociation of CH₄-rich hydrate. Regarding the CO₂/(CO₂ + N₂) ratio during step-wise depressurization, Fig. 2b shows upward trends until passing CO₂ HSZ. This could be justified by the fact that, during depressurization N₂-rich gas was removed, and consequently overall CO₂/(CO₂ + N₂) ratio was increased as a consequence of dissociation of those hydrates with more CO₂ than N₂, and after passing CO₂ HSZ this ratio reached to its maximum amount because of the dissociation of CO₂-rich hydrate. The maximum peak of this graph could be used as an indicator of efficiency of the CO₂ capture at the optimum pressure, in that more CO₂ stored at the optimum pressure means more CO₂ trapped in hydrate phase so that this peak will be higher because of dissociation of more CO₂ hydrate.

Effect of hydrate reservoir temperature on CO₂ sequestration. Both methane recovery and CO₂ storage strongly depend on hydrate reservoir temperature. The extent of changes in gas compositions at lower temperatures are typically larger than those at higher temperatures, as would be expected due to the stronger selectivity of CO₂ to N₂ and CH₄ in hydrate phase at lower temperature that dominates the molecular exchange between the gas and hydrate phase. In addition, the experimental pressures for lower temperatures were also lower than those for higher temperatures (see EXPERIMENTAL SECTION) due to the fact that hydrate dissociation points have lower pressures at lower temperatures. As a result, the compression cost for the reservoir with lower temperatures could be considerably lower. Although, lowering the temperature increases the time required for the process after ($t_{1/2}$), graphs for both methane recovery and CO₂ storage at negative temperatures show better efficiency in terms of time than positive ones at any times. With this in mind, the experiment at 261.2 K has the maximum efficiency for both methane recovery and CO₂ storage, indicating that the more CO₂ storage the more methane production. To be able to quantitatively analyse the results, C-value, is defined and referred to as the molar ratio of stored CO₂ in the hydrate phase after reaching equilibrium at target pressure to the injected total CO₂. C-value is calculated for each experiment using our in house thermodynamic modelling software³⁰ and is plotted in Fig. 3 together with CH₄ concentration in gas phase at target pressure after reaching equilibrium, before passing CH₄ HSZ, and before passing CO₂ HSZ. As can be seen 81.9% of the injected CO₂ present in the flue gas was stored in the hydrate phase at -12 °C, and the molar percentage of CH₄ in the gas phase reached 60.65, 93.34, 98.18 at the optimum pressure, and the boundary of CH₄ HSZ and CO₂ HSZ, respectively. For the experiments at higher temperatures, however, the figures in Fig. 3 decreased and reached a minimum in Experiment 7.

Response of CO₂-mixed hydrates to temperature rise. Thermal stability of the stored CO₂ is also a major issue for the long-term stability of the CO₂ underground because the temperature cycle in the storage environment may change the gas hydrates. This was the main reason for the investigation into the dissociation of hydrates in Experiment 2 R using thermal stimulation in addition to investigating the repeatability of the procedure. As can clearly be seen in Fig. 2, before depressurization Experiments 2 and 2 R showed very repeatable

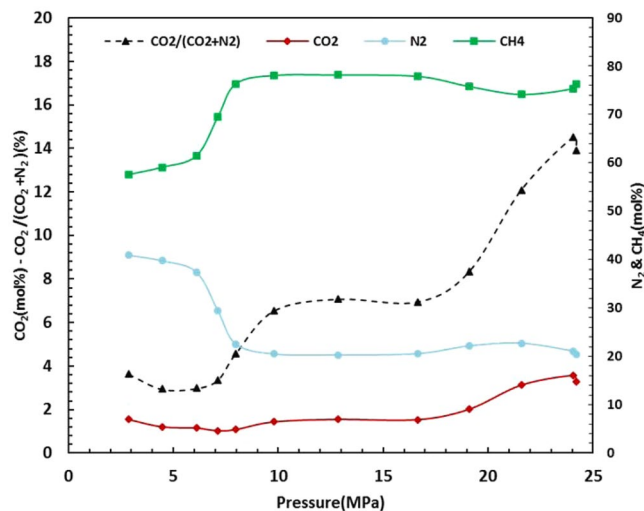


Figure 4. Gas compositional changes with pressure after cryostat temperature was set to 294.15 K at Experiment 2 R.

results. As mentioned before for Experiment 2 R, the temperature of the system was increased to investigate the dissociation behaviour of the previously formed hydrates at the optimum pressure. The gas composition evolution during dissociation was analysed by GC and the compositional results are plotted versus pressure in Fig. 4. As a result of temperature rise the gas phase starts to expand and the formed hydrates start to dissociate, which in turn leads to changes in the composition of the gas phase. As shown, initially the concentration of N₂ increases whereas the concentrations of CH₄, and CO₂ and CO₂/(CO₂ + N₂) reduces. The reduction of CO₂/(CO₂ + N₂) shows that initially those hydrates with relatively more N₂ start to decompose. This is a positive sign as it shows N₂ not only acts as promoting agent for CO₂/CH₄ replacement but also provides another safety factor for retention of the CO₂-rich hydrates during temperature rise. We have previously showed³¹ the role of N₂ for providing safety factor for thermal stability of stored CO₂ by hydrate formation using flue gas in absence of initial methane hydrate in place. However, this is the first mention of the potential safety role of N₂ for methane recovery by flue gas injection. After this phase, there is a sharp change in the composition of the gas phase before reaching an almost stable composition. In this period, the gas hydrates are quickly dissociating and the released gas is going to the gas phase, thus, the absence of changes in the gas phase implies that the composition of the gas phase in this period is similar to the composition of those hydrates which are dissociating. After this phase, there is another sharp increase followed by a slight decrease in CO₂ concentration and CO₂/(CO₂ + N₂) ratio before the system reaches equilibrium. This rise shows that hydrates with higher CO₂ content dissociate after dissociation of hydrates with lower CO₂ content. The possible explanation for the slight decrease in the concentration of the CO₂ and CO₂/(CO₂ + N₂) ratio is the higher solubility of CO₂³² compared to N₂ and CH₄.

Experimental Section

Materials. Deionized water (total organic carbon < 5 ppb) from an ELGA DV 25 Integral Water Purification was used for wetting sands, and cleaning of the experimental setup. The following gases from BOC Limited were used in the experiments: CO₂ (99.995 vol %), N₂ (99.995 vol %), and CH₄ (99.995 vol %). Well-characterized sands from Fife, Scotland were used for simulating mesoporous hydrate reservoirs. As described in our previous work³¹, the Sand mainly consists of quartz which has very small gas adsorption capacity³³ compared to gas inclusion in clathrate hydrate and water. Accordingly, the effect of gas adsorption to the sand was neglected in this study.

A high-pressure cylindrical cell setup was employed in all the experiments as shown in Fig. 5. The cell body is made of 316 stainless steel. The geometric area exposed to the hydrate-bearing sediments has been placed between a fixed top cap and a bottom cap. A movable piston is mounted above the bottom cap to simulate the overburden pressure, moving up and down by withdrawal or injection of hydraulic fluid behind the piston. Thus, the reservoir is not in direct contact with hydraulic fluid. Hydraulic fluid injection/removal was performed using a dual-cylinder Quizix pump (SP-5200, Chandler Engineering) for maintaining the pressure or a hand pump for achieving initial compaction pressure. A linear variable differential transformer (LVDT) is mounted on the bottom cap to measure the piston movement; therefore, the reservoir volume could be calculated at any stage. For controlling the temperature during experiments, the cell is fitted in an aluminium jacket, which is cooled/heated as a whole by circulation of the cooling fluid (water/monoethylene glycol solution from a cryostat (Julabo MA-4). The cooling jacket is wrapped with an insulation layer to reduce the heat transfer from the surrounding environment and the temperature gradient. Two QUARTZDYNE pressure transducers (model QS30K-B, Quartzdyne Inc., U.S.A.) (+/- 0.005 MPa) and a Platinum Resistance Thermometer (PRT) (+/- 0.1 K) were used to measure the cell and overburden pressures, and the cell temperature, respectively. The temperature, all pressures (including pore pressure, overburden pressure, and pump pressure), and the LVDT displacement were monitored by a feedback system of the setup (LabVIEW software from National Instruments). All gas injections, withdrawals, and

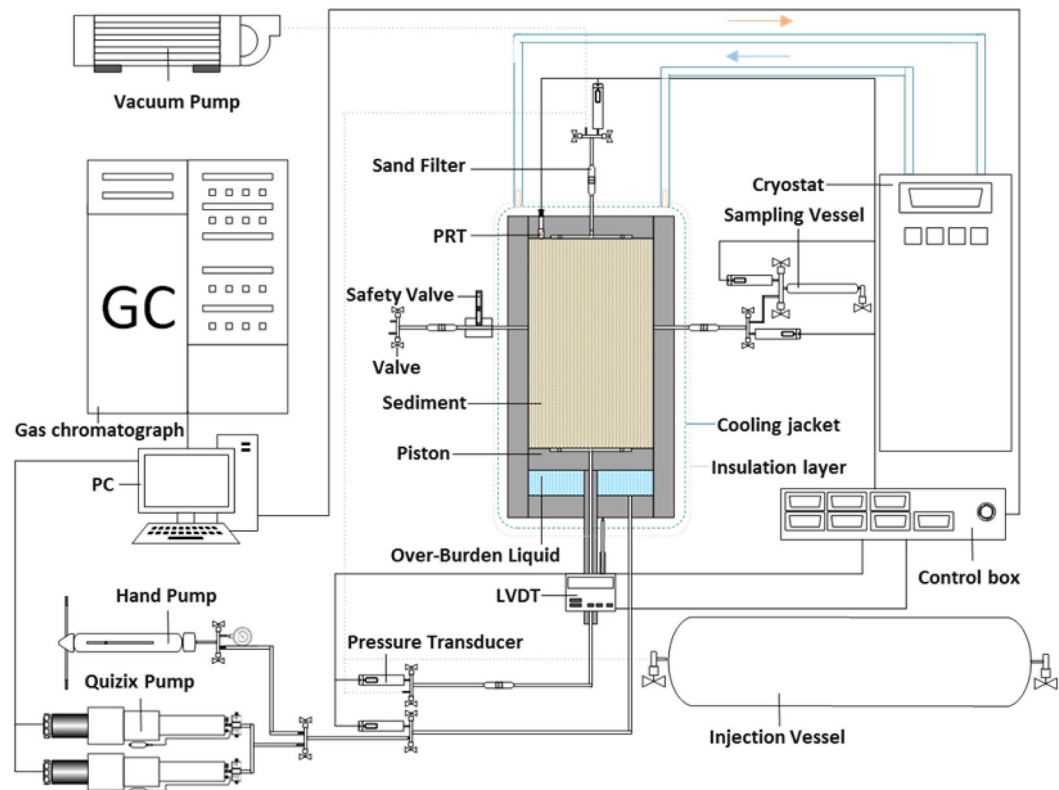


Figure 5. Schematic of the high-pressure cell setup.

sampleings, were achieved using valves allocated at the top, bottom, and two sides. Finally, a Gas Chromatograph (GC) (Varian 3600, Agilent Technologies) was used to analyse the composition of gas samples for monitoring the evolution in gas composition within the system.

Procedure. In a typical test, 1076.6 g of the sand was partially saturated with 155.6 g deionized water. The wetted sediment was then loaded into the cell, and the system was evacuated to soak the remained air out. Following evacuation, the piston level was adjusted to compact the system with 3.45 MPa overburden pressure for at least a day. Prior to injection of the test gas, the system temperature was set to 298.15 K (to ensure there was no hydrate formation possibility in the working pressure range). A certain amount of CH₄ gas was then added through the valves from top and bottom until the desired initial pressure is reached. Subsequently, the system temperature was set to 273.35 K (just above freezing point of water) to form hydrate without appearance of ice in the system. The system pressure reduced as temperature declined. Since water was exposed to the high pressure CH₄ well inside the HSZ at this point, hydrate formation started, reducing the system pressure till the equilibrium point was reached at the experimental temperature. The onset of hydrate formation appeared at the point where there was a clear change in slope of the pressure profile during cooling. The hydrate formation period could take more than a week because there was no mixing in the system. Although some conventional temperature cycling methods (e.g. Stern's method³⁴) could be used to accelerate the hydrate formation, the cryostat temperature remained stable to preserve the sediment structure built in an entirely controlled method. Hydrate formation/growth continued until a stable pressure profile could be observed, confirming completion of hydrate formation.

After completion of hydrate formation, the first test was conducted at this hydrate formation temperature while for the other experiments, the bath temperature was re-set to the target temperature. At this point, hydrate, gas, water, and ice saturation were calculated as shown in Table 1. The same formulation as our previous work³⁵ was used for the calculation of the saturation. For purging the remaining methane gas and reducing the proportion of remaining free methane in the gas phase without dissociation of methane hydrate, flue gas composed of 85.4 mol % N₂ and 14.6 mol % CO₂ was injected to the cell at a pressure approximately 10 times the equilibrium pressure of methane hydrate at the target temperature after hydrate formation. Then gas was slowly released from the system until the system was depressurized to 0.7 MPa above flue gas hydrate phase boundary immediately to avoid or minimise formation of flue gas hydrates. Once the methane concentration was less than 15% during the purging process, the injection port was closed and the system pressure was reduced to a specified optimum point by moving the piston backward. These optimum pressures were determined by the method described in the companion paper to this work¹⁰. At this step, pressure was maintained using a dual-cylinder Quizix pump and samples from the gas phase were collected at pre-determined time intervals to be analysed using a GC. After reaching the equilibrium condition (no change in gas composition for 3 days), the system was depressurized in a stepwise manner to recover the remaining methane. Experiment 2 R was conducted to check the repeatability

Experiment No.	1	2	3	4	5	6	7	2R
Temperature (K)	261.2	264.8	268.6	273.3	278.1	282.1	284.2	264.8
Hydrate saturation (vol%)	67.5	66.8	66.2	60.2	54.4	48.8	47.3	66.9
Gas saturation (vol%)	24.8	25.1	25.6	28.3	26.0	27.1	25.5	25.0
Water saturation (vol%)	0.0	0.0	0.0	11.5	19.6	24.1	27.2	0.0
Ice + Quasi liquid saturation (vol%)	7.7	8.1	8.2	0.0	0.0	0.0	0.0	8.1

Table 1. Hydrate, gas, water, and Ice + quasi liquid saturation after methane hydrate formation and before flue gas injection.

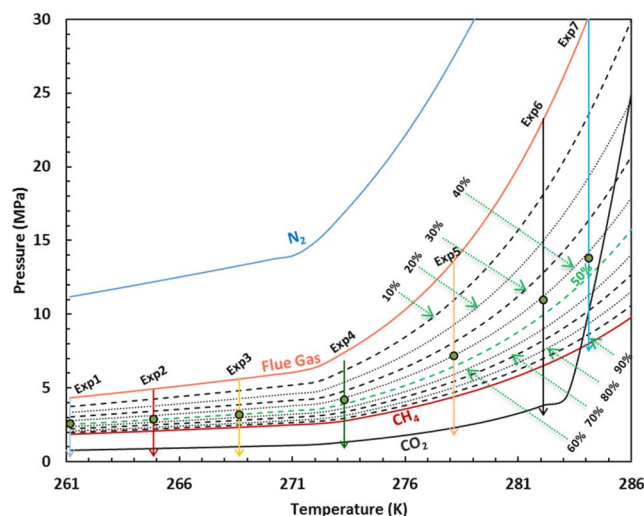


Figure 6. The predicted hydrate stability zones of CO_2 , N_2 , CH_4 and their mixtures and the experimental conditions.

of the experiments, which followed the same procedure as Experiment 2. However, after reaching equilibrium state at the target pressure, instead of depressurization, the system was heated to room temperature (294.15 K) to investigate dissociation of the formed hydrates.

As we have previously defined the effect of pressure on the CO_2 storage and methane recovery, and have indicated that there is an optimum pressure¹⁰ at each temperature using simulated bulk conditions, it is necessary to determine the efficiency of the method at real world conditions. Furthermore, it is also important to characterize the kinetics of the process in such conditions as mass and heat transfer is strongly constrained by mesoporous media. In addition, the effect of ice on the kinetics of the process was investigated to cover conditions of encountered in methane hydrate reservoirs located in high-latitude regions of the Earth. Hence, the experiments were designed to fundamentally understand the kinetics and efficiency of methane recovery and CO_2 storage by injection of flue gas into hydrate-bearing sediments at the previously defined optimum pressures. The procedure was in all cases as described above. The experimental pressure/temperature conditions together with hydrate stability zones of N_2 , CH_4 , CO_2 , flue gas, and different combinations of flue gas/ CH_4 are provided in Fig. 6. The green dots show the optimum conditions at which the system was kept at nearly constant pressure. According to Fig. 6, the experiments sufficiently cover a temperature range for permafrost, sub permafrost, subglacial, and subsea sediments³⁶.

Received: 14 May 2019; Accepted: 22 October 2019;
Published online: 07 November 2019

References

- Kvenvolden, K. A. & Lorenson, T. D. The Global Occurrence of Natural Gas Hydrate. *In Geophysical Monograph Series* **124**, 3–18 (2013).
- Yang, S. H. B., Linga, P., Chong, Z. R., Babu, P. & Li, X.-S. Review of natural gas hydrates as an energy resource: Prospects and challenges. *Appl. Energy* **162**, 1633–1652 (2015).
- House, K. Z., Schrag, D. P., Harvey, C. F. & Lackner, K. S. Permanent carbon dioxide storage in deep-sea sediments. *Proc. Natl. Acad. Sci.* **103**, 12291–12295 (2006).
- Sloan, E. D. Fundamental principles and applications of natural gas hydrates. *Nature* **426**, 353–359 (2003).
- Yin, Z., Moridis, G., Chong, Z. R., Tan, H. K. & Linga, P. Numerical Analysis of Experiments on Thermally Induced Dissociation of Methane Hydrates in Porous Media. *Ind. Eng. Chem. Res.* **57**, 5776–5791 (2018).
- Terzariol, M., Goldsztein, G. & Santamarina, J. C. Maximum recoverable gas from hydrate bearing sediments by depressurization. *Energy* **141**, 1622–1628 (2017).

7. Li, G. *et al.* Experimental Investigation into the Production Behavior of Methane Hydrate under Methanol Injection in Quartz Sand. *Energy and Fuels* **31**, 5411–5418 (2017).
8. Mery, S., Al-Raoush, R. I., Jung, J. & Alshibli, K. A. Comprehensive literature review on CH₄-CO₂ replacement in microscale porous media. *J. Pet. Sci. Eng.* **171**, 48–62 (2018).
9. Chen, Y. *et al.* Experimental investigation of different factors influencing the replacement efficiency of CO₂ for methane hydrate. *Appl. Energy* **228**, 309–316 (2018).
10. Hassanpouryouzband, A. *et al.* CO₂ Capture by Injection of Flue Gas or CO₂-N₂ Mixtures into Hydrate Reservoirs: Dependence of CO₂ Capture Efficiency on Gas Hydrate Reservoir Conditions. *Environ. Sci. Technol.* **52**, 4324–4330 (2018).
11. Hassanpouryouzband, A. *et al.* Insights into CO₂ Capture by Flue Gas Hydrate Formation: Gas Composition Evolution in Systems Containing Gas Hydrates and Gas Mixtures at Stable Pressures. *ACS Sustain. Chem. Eng.* **6**, 5732–5736 (2018).
12. Tupsakhare, S. S. & Castaldi, M. J. Efficiency enhancements in methane recovery from natural gas hydrates using injection of CO₂/N₂ gas mixture simulating *in-situ* combustion. *Appl. Energy* **236**, 825–836 (2019).
13. IPCC. Climate Change 2013 - The Physical Science Basis. Climate Change 2013 - The Physical Science Basis (IPCC, 2014), <https://doi.org/10.1017/cbo9781107415324>
14. Merkel, T. C., Lin, H., Wei, X. & Baker, R. Power plant post-combustion carbon dioxide capture: An opportunity for membranes. *J. Memb. Sci.* **359**, 126–139 (2010).
15. Yang, J. *et al.* Flue gas injection into gas hydrate reservoirs for methane recovery and carbon dioxide sequestration. *Energy Convers. Manag.* **136**, 431–438 (2017).
16. Peter, E., Messah, M. & Chau, J. Gas Recovery Through the Injection of Carbon Dioxide or Concentrated Flue Gas in a Natural Gas Hydrate Reservoir. in Offshore Technology Conference Asia, <https://doi.org/10.4043/28374-ms> (Offshore Technology Conference, 2018).
17. Li, B. *et al.* An experimental study on gas production from fracture-filled hydrate by CO₂ and CO₂/N₂ replacement. *Energy Convers. Manag.* **165**, 738–747 (2018).
18. Mu, L. & Von Solms, N. Experimental Study on Methane Production from Hydrate-Bearing Sandstone by Flue Gas Swapping. *Energy and Fuels* **32**, 8167–8174 (2018).
19. Okwananke, A. *et al.* Methane recovery from gas hydrate-bearing sediments: An experimental study on the gas permeation characteristics under varying pressure. *J. Pet. Sci. Eng.* **180**, 435–444 (2019).
20. Wang, X. *et al.* Reservoir volume of gas hydrate stability zones in permafrost regions of China. *Appl. Energy* **225**, 486–500 (2018).
21. Lin, Z., Pan, H., Fang, H., Gao, W. & Liu, D. High-altitude well log evaluation of a permafrost gas hydrate reservoir in the Muli area of Qinghai, China. *Sci. Rep.* **8**, 12596 (2018).
22. Boswell, R. *et al.* Permafrost-associated natural gas hydrate occurrences on the Alaska North Slope. *Mar. Pet. Geol.* **28**, 279–294 (2009).
23. Geng, C. Y., Wen, H. & Zhou, H. Molecular simulation of the potential of methane reoccupation during the replacement of methane hydrate by CO₂. *J. Phys. Chem. A* **113**, 5463–5469 (2009).
24. Bai, D., Zhang, X., Chen, G. & Wang, W. Replacement mechanism of methane hydrate with carbon dioxide from microsecond molecular dynamics simulations. *Energy Environ. Sci.* **5**, 7033–7041 (2012).
25. Lee, B. R., Koh, C. A. & Sum, A. K. Quantitative measurement and mechanisms for CH₄ production from hydrates with the injection of liquid CO₂. *Phys. Chem. Chem. Phys.* **16**, 14922–14927 (2014).
26. Dornan, P., Alavi, S. & Woo, T. K. Free energies of carbon dioxide sequestration and methane recovery in clathrate hydrates. *J. Chem. Phys.* **127**, 124510–124700 (2007).
27. Petuya, C., Damay, F., Chazallon, B., Bruneel, J. L. & Desmedt, A. Guest Partitioning and Metastability of the Nitrogen Gas Hydrate. *J. Phys. Chem. C* **122**, 566–573 (2018).
28. Chazallon, B. & Pirim, C. Selectivity and CO₂ capture efficiency in CO₂-N₂ clathrate hydrates investigated by *in-situ* Raman spectroscopy. *Chem. Eng. J.* **342**, 171–183 (2018).
29. Koh, D. Y. *et al.* Recovery of methane from gas hydrates intercalated within natural sediments using CO₂ and a CO₂/N₂ gas mixture. *ChemSusChem* **5**, 1443–1448 (2012).
30. Mahabadian, M. A., Chapoy, A., Burgass, R. & Tohidi, B. Development of a multiphase flash in presence of hydrates: Experimental measurements and validation with the CPA equation of state. *Fluid Phase Equilib.* **414**, 117–132 (2016).
31. Hassanpouryouzband, A. *et al.* Geological CO₂ Capture and Storage with Flue Gas Hydrate Formation in Frozen and Unfrozen Sediments: Method Development, Real Time-Scale Kinetic Characteristics, Efficiency, and Clathrate Structural Transition. *ACS Sustain. Chem. Eng.* <https://doi.org/10.1021/acssuschemeng.8b06374> (2019).
32. Hassanpouryouzband, A. *et al.* Solubility of Flue Gas or Carbon Dioxide-Nitrogen Gas Mixtures in Water and Aqueous Solutions of Salts: Experimental Measurement and Thermodynamic Modeling. *Ind. Eng. Chem. Res.* **58**, 3377–3394 (2019).
33. Stahl, W., Faber, E., Carey, B. D. & Kirksey, D. L. Near-surface evidence of migration of natural gas from deep reservoirs and source rocks. *Am. Assoc. Pet. Geol. Bull.* **65**, 1543–1550 (1981).
34. Stern, L. A., Kirby, S. H. & Durham, W. B. Peculiarities of methane clathrate hydrate formation and solid-state deformation, including possible superheating of water ice. *Science (80-)*. **273**, 1843–1848 (1996).
35. Yang, J. *et al.* Gas hydrates in permafrost: Distinctive effect of gas hydrates and ice on the geomechanical properties of simulated hydrate-bearing permafrost sediments. *J. Geophys. Res. Solid Earth* **124**, 2551–2563 (2019).
36. Portnov, A., Vadakkepuliambatta, S., Mienert, J. & Hubbard, A. Ice-sheet-driven methane storage and release in the Arctic. *Nat. Commun.* **7** (2016).

Acknowledgements

This work was financially supported by the Skolkovo Institute of Science and Technology, Russia, which is acknowledged gratefully. The experiments were conducted at the Centre for Hydrate Research, Institute of Petroleum Engineering, Heriot-Watt University, Edinburgh, United Kingdom.

Author contributions

A.H., J.Y. and A.O. conceived the idea presented in this publication; A.H., A.O. Performed laboratory experiments and analysed the data; B.T. and J.Y. supervised the research; A.H. and J.Y. Wrote the manuscript. R.B., B.T., E.C., V.I. and B.B. discussed the results and contributed to the final manuscript.

Competing interests

The authors declare no competing interests.

Additional information

Correspondence and requests for materials should be addressed to J.Y.

Reprints and permissions information is available at www.nature.com/reprints.

Publisher's note Springer Nature remains neutral with regard to jurisdictional claims in published maps and institutional affiliations.



Open Access This article is licensed under a Creative Commons Attribution 4.0 International License, which permits use, sharing, adaptation, distribution and reproduction in any medium or format, as long as you give appropriate credit to the original author(s) and the source, provide a link to the Creative Commons license, and indicate if changes were made. The images or other third party material in this article are included in the article's Creative Commons license, unless indicated otherwise in a credit line to the material. If material is not included in the article's Creative Commons license and your intended use is not permitted by statutory regulation or exceeds the permitted use, you will need to obtain permission directly from the copyright holder. To view a copy of this license, visit <http://creativecommons.org/licenses/by/4.0/>.

© The Author(s) 2019